International Journal of Nanoelectronics and Materials

In Press, Accepted Manuscript – Note to user

Microbial activity of TiO2 NPs via two phases Synthesized by the sol-gel method

Firas. H. Ibrahim[1*], Olfat Mahmoud[1]

[1]Department of physics, Scince of college, University Diyala, Iraq.

Received 16 May 2022, Revised 5 August 2022, Accepted 16 August 2022

ABSTRACT

TiO_2 titanium dioxide nanophases of anatase and rutile were controlled only by temperature control of the calcination process, which is a cheap technical technique, and were organized using a sol-gel process, which involved mixing titanium tetrachloride ($TiCl_4$) with ethanol as starting materials, as well as heating at various temperatures (650, 850 ℃). The fundamental properties of the as-prepared nanomaterials were investigated using Fourier transform infrared spectra (FTIR). The antibacterial activity of TiO_2 was next investigated using two strains of E. coli, Staphylococcus aureus, and Streptococcus bacteria. The TiO_2 structure has a dominating phase of 650 °C in addition to rutile at 850 °C, with an average volume of crystalline (D) of 21.9 nm for the anatase phase and 30.41 nm for the rutile phase. According to XRD data, the spherical shape of the rutile phase is clearly evident in the TEM of TiO_2 NPs, the tetragonal shape is clearly seen in the anatase, and the calcination process had a major effect on the crystal size. According to FTIR analysis, the majority of peaks are seen between 400 and 700 cm-1 as a result of bending and oscillation lengthening. The studies demonstrated that TiO_2, in both protease and rutile forms, is a highly efficient antibacterial that can be used as a self-cleaning exterior to exterior surfaces (windows) as well as in bio-penetration places like hospitals and medical clinics.

Keywords: TiO_2 NPs – Sol gel method - antimicrobial properties.

1. INTRODUCTION

Nanotechnology is an applied science discipline concerned with the design, manufacture, characterization, and application of nanoscale materials. It is a discipline of research that contains a sub-category for colloidal knowledge, as well as the study of phenomena and doctrinaire of nanoscale materials in physics, chemistry, biology, and other scientific areas [1, 2]. Their photocatalyst is one-of-a-kind properties TiO_2 nanoparticles are interesting by scaling. As a result, this increased its role in understanding, creating and improving materials for different applications. TiO_2 has been widely for many technological and as antibacterial agents' applications [3-5]. Titanium dioxide crystals exist in nature in three polymorphs: rutile, anatase, and [6] temperatures less than 600 °C, whereas the two phases (rutile and brookite) are generated at high temperatures [7]. Titanium dioxide (TiO_2) is being studied extensively for its ability to remove organic contaminants from various media. Furthermore, the TiO_2 nanoparticle actual activity in the Gram-positive strain assay, such a bacteria-resistant variation of both The properties of nanoparticles - gram-negative and gram-negative - can be explained by selling intermediate conditions possibly favoring the delayed closing interface of the nanoparticles and the Gram-positive microbial cell, which can also improve its binding to the external anchor microbial cells, It also has a one-of-a-kind photocatalytic activity, good thermal stability, and chemical biocompatibility. Surface chemistry, such as the quantity of surface flaws, is known to govern TiO_2 NPs antibacterial activity, which has a significant impact on the particles' photocatalytic activity [8-12].

*Corresponding author: sciphyms19@uodiyala.edu.iq

In various studies, TiO_2 has been combined with a variety of nanomaterials to act as an antibacterial agent. For example, Fe_3O_4-TiO_2 core/shell NPs were created to inhibit the growth of Staphylococcus aureus, which had a survival ratio of 82.4 percent before treatment and 7.13 percent after treatment. The survival ratio of Escherichia coli bacteria was reduced by 97.53 percent when TiO_2 nanotubes were utilized to confine them [13]. TiO_2 can be used in coatings [14], water purification, power and air purification [15], medicine [16], food products [17], cosmetics [18] Photocatalysis. TiO_2 nanoparticles can be synthesized using different techniques such as sulfate process [19], hydrothermal method [5, 20], The chemical mechanism for making TiO2 nanoparticles is called sol–gel synthesis. The sol–gel production of TiO_2 nanoparticles is a procedure in which TiO_2 is extracted from condensed titanium hydroxide in a gel [21, 22], In terms of purity, homogeneity, and stoichiometry control, the sol–gel process outperforms alternative fabrication techniques. The size of TiO_2 particles is determined by grain size, impurities, composition, and calcination temperatures [23, 24]. The size, stability, and concentration of TiO_2 NPs in the growth medium impact their bactericidal characteristics, which allows for a longer retention time for bacterium NP interaction, allowing them to engage closely with microbial membranes [25, 26]. This paper discusses the influence of calcination temperature on the phase shift of two-phase titanium dioxide nanoparticles, which are produced using a modified sol-gel process. The solubility of the reagents in the solvent determines the gel's homogeneity. Particles are characterized using (XRD), (TEM), and (FTIR) equipment. The goal of this paper is to use the sol-gel method to make TiO_2 NPs with two phases of anatase and rutile and then tested with a variety of diseases, including E. coli, Staphylococcus aureus, and Streptococcus bacteria. On cultures of gram-negative and gram-positive bacteria, TiO_2 NPs with and without amoxicillin were tested for antibacterial activity.

2. EXPERIMENTAL METHOD

2.1 Materials and method for preparing and imposing nanoparticles

Ethanol CH3CH2OH (99.99%) and titanium tetrachloride $TiCl_4$ (99.99%) were determined as raw materials for the production of TiO_2 NPs by adding $TiCl_4$ dropwise to ethanol at a ratio of 2:20 due to the large amounts of Cl_2 and HCl in the reaction, complete at room temperature with "stirring" under a fume hood. A pale-yellow liquid is absorbed and transformed into gelatin in order to express an aqueous gel solution. The pH is 1.4. As a result, the sol-gel solution was evaporated at 85 °C until it became a dry gel. In a box heater, the starting material was dry-gel calcined for 2 hours at various temperatures (650, 850) °C. The anatase and rutile phases of TiO_2 were obtained using the calcination procedure. The anatase phase is achieved within a period of (2-2) hours at a temperature of (650) °C. On the other hand, the rutile phase is reached within (2-2) hours at (850) °C. Results are reported in the literature [2]. X-ray diffraction was used to determine crystal phases and to estimate crystal size. The size and shape of the nanoparticles were examined using transmission electron microscopy (TEM), and Fourier transform infrared spectroscopy to determine the chemical limits of the substance at the wave number in the range of (400–4500) cm^{-1}.

2.2 Antimicrobial activity of TiO2 NPs

Gram-positive bacteria (*Streptococcus and Staphylococcus aureus*) and gram-negative bacteria *E. coli* were chosen as the standard bacterial contaminants for this study. Bacterial strains were achieved through evaluation in addition to the diagnostic laboratory in Muqdadiya General

Hospital, Diyala, Iraq. Bacteria were cultured on nutrient agar (N. hach) for 24 hours at 37 °C. In addition to the transverse amplitudes that were then surrounded and measured in millimeters, the fine diffusion method was used by spreading the bacterial grass on the nutrient agar plates and leaving them for a few minutes. Using a piercing gel, circles of 6 mm in diameter were created on the nutrient agar plate. Each single pressure piece is inoculated onto a dedicated plate with a sterile cotton swab using different models of micropipettes, after adding TiO_2 NPs phases (TiO_2 Anatase) and (TiO_2 Rutile), at different concentrations (400, 600, and 200) µg mL-1 and transferring accurate nanoparticles every minute over the entire plate. Additionally, use microcenter plates for continuous control of water. Then, they were varnished at a designated 37 °C for 24 h, and waited for efficacy assessment areas after the operation. The effect of TiO_2 NPs was evaluated at (600 µg mL-1) with amoxicillin (30 µg mL-1). For the same types of *E. coli, Streptococcus, and Staphylococcus aureus* using the agar diffusion method, 9 mm wells were drilled in agar using a sterile cotton swab, and a mixing solution of TiO_2 NPs and amoxicillin was poured into the hole. The inhibitory activity was monitored after the incubation process to evaluate the efficiency of the TiO_2 NPs phase (TiO_2 Anatase) and (TiO_2 Rutile) with and without amoxicillin by measuring the diameters of the inhibition zone from different directions more than once using a ruler.

3. RESULTS AND DISCUSSION

(XRD) patterns of calcined titanium oxide (TiO_2) at two different temperatures (650 and 850) °C, which is the crystal structure of the rutile and anatase types, are shown in figure 2. The results showed that TiO_2 was revealed as rutile at a temperature of (850 °C) with a tetragonal crystalline structure with a crystalline plane of (P42/mnm no.136), crystal dimensions (a = b = 4.566, c = 2.948 ˚A) and angles (α=β=γ= 90°), which are in agreement with the standard card (JCPDS 08-5492). Titanium dioxide-anatase type, with a tetragonal crystalline structure with a crystalline plane of (I 41/amd no. 141), crystal dimensions of (a=b=3.77, c= 9.42 ˚A) and angles (α=β=γ= 90°) was at a temperature of (650°C). which is in agreement with the standard card (JCPDS 15-4609). The Nano-Anatase phase was obtained at a temperature of 650 °C. At this temperature, this phase becomes clearer and crystallizes, where the diagnostic peaks become sharper and more distinct. Using the Debye-Scherrer's equation, the average crystal size of titanium dioxide (TiO_2) was estimated to be (30.41 nm) and (21.4 nm) at temperatures (650 °C) respectively, which shows an increase in crystalline size with an increase in temperature due to an increase in crystalline growth with increasing temperature and consequently an increase in crystal size [27], as shown in Tables 1 and 2 that summarize the crystal size values and some constants for the prepared samples at different temperatures.

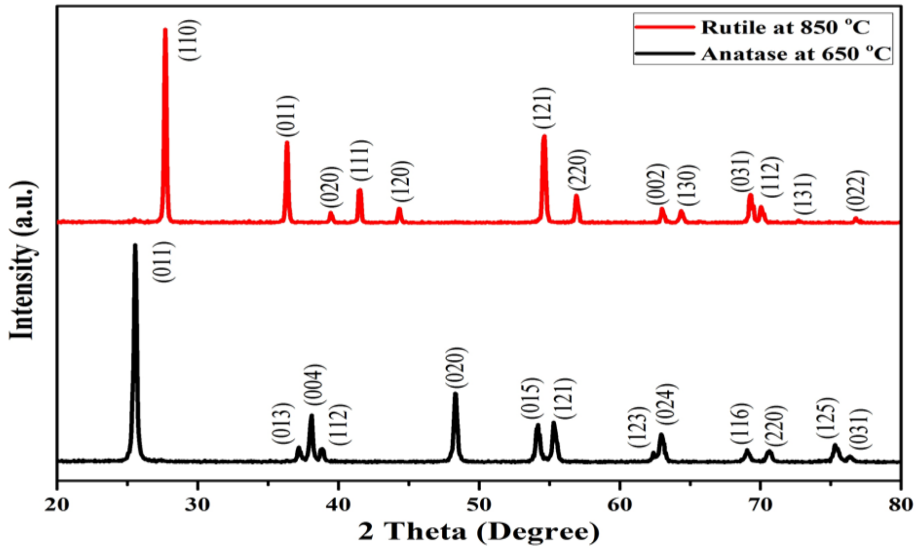

Figure 1. X-ray diffraction of calcined titanium oxide (TiO_2) at different temperatures (650, 850 °C).

Table 1 X-ray diffraction calculations for titanium oxide (TiO_2), a type of calcined rutile at a temperature of (850°C).

2Ө (deg) Practical	2Ө (deg) Standard	FWHM (deg)	Crystalline size (nm)	dhkl (°A) Practical	dhkl (°A) Standard	(hkl)
27.65	27.6	0.2011	38.359	3.223	3.228	(110)
54.66	54.63	0.2691	26.22	1.677	1.678	(121)

Table 2 X-ray diffraction calculations for titanium oxide (TiO2), anatase type, calcined at (650 °C).

2Ө (deg) Practical	2Ө (deg) Standard	FWHM (deg)	Crystalline size (nm)	dhkl (°A) Practical	dhkl (°A) Standard	(hkl)
25.58	25.42	0.28323	27.35	3.479	3.5001	(011)
48.31	48.24	0.30896	23.46	1.882	1.885	(020)

At heating of TiO_2 rutile to 850 °C, the bands linked to the stretching of the-CH_2 and-CH_3 groups were seen at roughly 2362 cm^{-1} in the spectra (black curve), those observed below 3000 cm^{-1} because of the ethyl groups' asymmetric and symmetric stretching vibrations, respectively [28-30]. In my spectrum, the bands related to the C–O groups (TiO_2 anatase) and (TiO_2 rutile) are represented by black and red curves at 1387 and 1167 cm^{-1}, respectively [29, 30], while the asymmetric stretching of the OH groups is represented by a strong intensity band at 3743 cm^{-1}.

The strong bands related to the bending scissoring H-O-H vibration can be seen at 1548 cm^{-1} and 1523 cm^{-1} in the black and red curves, respectively. The presence of weakly bound water determines the position and structure of this band, which is further supported by the band at 1650 cm^{-1} [31]. The signals between 1000 and 400 cm^{-1} are caused by the bending vibrations of Ti–OH and Ti–O, O–Ti–O bonds [32].

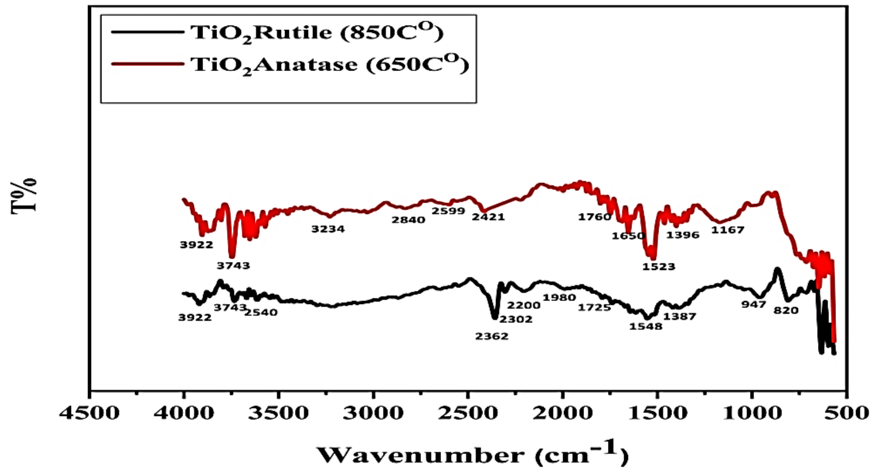

Figure 2. FTIR spectra of all synthesized nanoparticles at different temperatures.

The NPs size and shapes for anatase phase and rutile phase NPs prepared by using $TiCl_4$ precursor and the sol-gel process can determine the shape and size of anatase NPs in the range of 100 nm with hexagonal uniform and spherical homogenous particles. The tetragonal shape is clearly seen, and these results agree with [28]. As previously said, the anatase phase container uses fashionable coating in arrears of photocatalytic properties that make such things as self-cleaning surfaces and materials, and this homogeneity enables such particles' effects on the local coating when added. Figure 4 depicts the morphology and measurements of TiO_2 NPs in rutile TiO_2, having elliptical forms and in the range of 100 nm. Images of TiO2 nanoparticles taken by using (TEM) as shown in Figure (3) and (4). It was discovered that increasing the calcination temperature causes the size of the particles and the crystal size of the TiO2 particles to rise. This is due to an increase in crystal accumulation, which resulted in a decrease in surface area and an increase in crystal size. This demonstrates that the anatase phase exists at the calcination temperature (650 °C) At the scale 100 nm it shows the statistical distribution of the particle diameters (TiO2 Anatase) and it appears from the drawing that the nanoparticles' diameters are centered at (15.419) nm, as seen in picture (3). The calcination temperature (850 °C) was turned into phase for the rutile trip with a visit to the temperature at the scale 100 nm it shows the statistical distribution of the particle diameters (TiO2 Rutile) and it appears from the drawing that the nanoparticles' diameters are centered at (37.05) nm, as shown in Figure (4). The first process is for nanoparticles of tiny size, while the second procedure is for nanoparticles of large size [29]. TEM images confirmed that the manufacture of the powder phase (TiO_2) strongly depends on the high temperature of calcining. These (TEM) results agree well with the XRD results in Figure 1, where it is shown that the widest peaks of the XRD at the temperature calcined (850°C), where the crystallization of (TiO_2) was found to be indicative of the sharper and narrower peaks of the XRD patterns, This agrees with researcher Siripond Phromma [30].

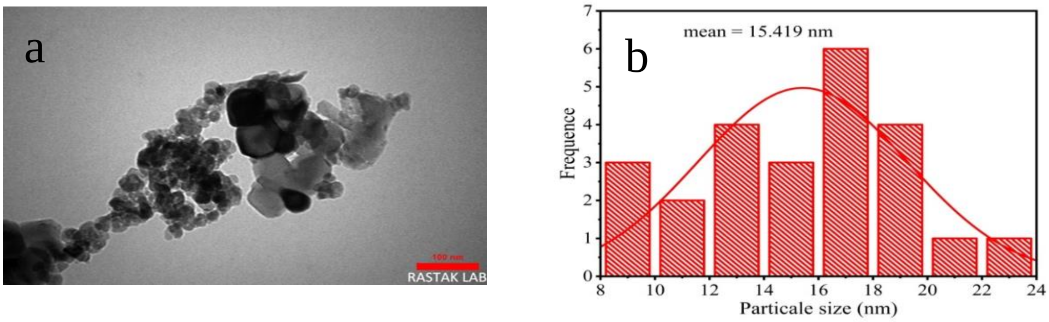

Figure 3. (a) Transmission electron microscopy (TEM) image of (TiO2 Anatase) at calcined temperature (650 °C). (b) Statistical distribution of particulate matter (TiO2 Anatase) at a wide.

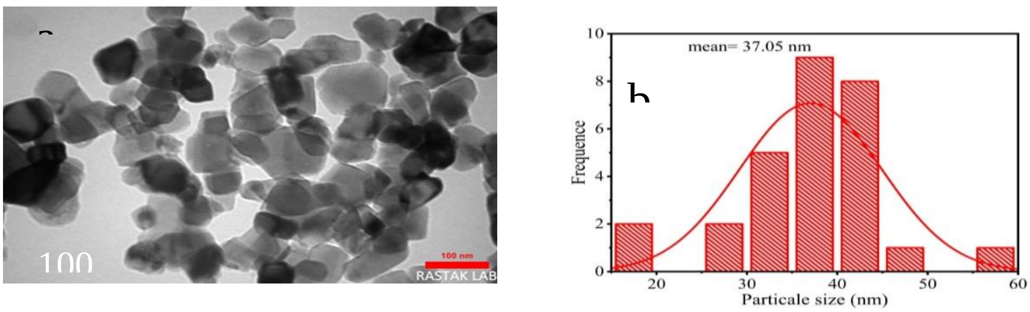

Figure 4. (a) Transmission electron microscope (TEM) image of (TiO_2 Rutile) nanoparticles at calcined temperature. (850°C), (b)Statistical distribution of particles (TiO_2 Rutile) at scale.

That 600 µg mL^{-1} of (TiO_2 Anatase) and (TiO_2 Rutile) NPs was found to be the most effective concentration for limiting evolution of all the chains. For Escherichia coli, Streptococcus, and Staphylococcus aureus, s shown in figure (5), the case of the antibacterial well diameter is distinguished, as the diameters are in the form of (6 mm and 9 mm), which includes antibacterial well models, but if the antibacterial diameter is equal to or minus 6 mm and 9 mm thick, the specimen has secondary antimicrobial properties. Complete models showed increased antibacterial activities of the circular diameters and antibacterial abundance greater than 6 mm by 9 mm, Table (3) shows the region of inhibition of TiO_2 NPs against pathogens under visible light. fig. Figure 6 shows a fine diffusion assay for TiO_2 NPs. Sample (S1, S2, S3) representative of TiO2 Anatase NPs at 200 µg mL^{-1} shows sensitivity to bacteria (23 mm), (19 mm), and (8 mm) against E. coli bacteria (S1), Streptococcus (S2), and Staphylococcus aureus (S3), respectively. The area of inhibition at 400 µg mL^{-1} was (24 mm), (22 mm) and (9 mm) against pathogens (*E. coli, Streptococcus and Staphylococcus aureus*) respectively and the area of inhibition of TiO_2 NPs was at 600 µg mL^{-1}. (28 mm), (25 mm) and (12 mm) respectively on the same bacterial species, While the sample (X1, X2, X3) representing TiO_2 Rutile NPs on the same bacteria shows an inhibition area at 200 µg mL^{-1} sensitivity to bacteria (21 mm), (18 mm), and (6 mm) respectively against Escherichia bacteria coli (X1), Streptococcus (X2), and Staphylococcus aureus (X3), respectively. The area of inhibition at 400 µg mL^{-1} was (23 mm), (19 mm) and (9 mm) against pathogens (*E. coli, Streptococcus and Staphylococcus aureus*) respectively and the area of inhibition of TiO_2 NPs was at 600 µg mL^{-1}. (24 mm), (21mm) and (11mm) respectively for the same bacterial species, Figures (6-a-b) show that sample S1, S2 and S3 (TiO_2 Anatase) have much higher antibacterial activity than samples X1, X2 X3 results are reported (TiO_2 rutile) in the literature [28]. When the degree of calcination of TiO_2 NPs increases, the particle size increases, which reduces its antibacterial activity. Good agreement with the results of (XRD).

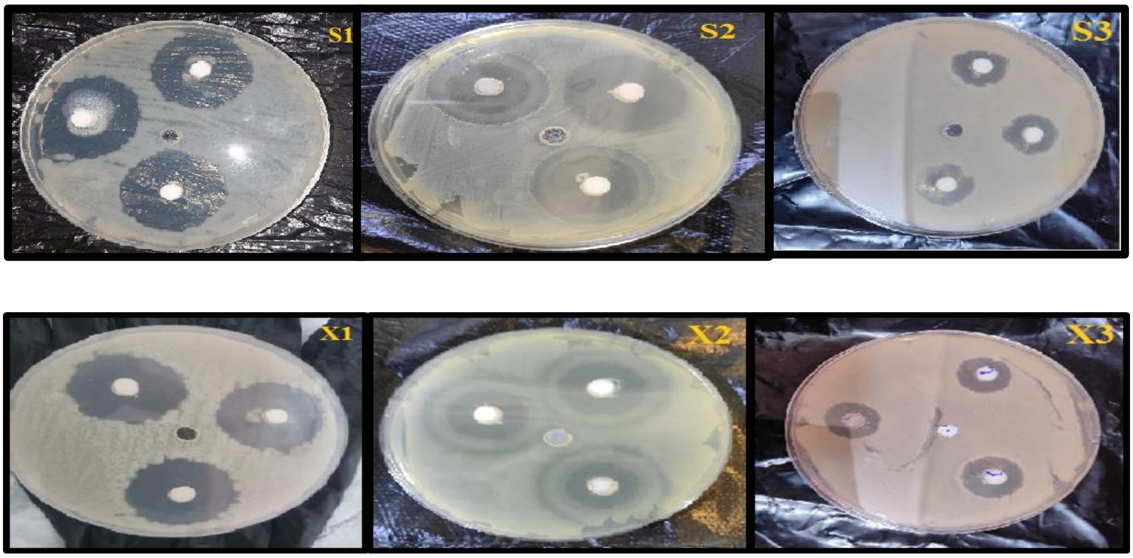

Temp.°C	Phase TiO2	Microorganism	Zone of inhibition, mm			
			200µg mL^{-1}	**400µg mL^{-1}**	**600µg mL^{-1}**	**Control**
650°C	**Anatase (S1 ,S2 ,S3)**	***E. coli***	23	24	**28**	**-**
		Streptococcus mutans	**19**	**22**	**25**	**-**
		Staphylococcus aureus	8	9	12	**-**
850°C	Rutile **(X1, X2, X3)**	***E. coli***	21	23	**24**	**-**
		Streptococcus mutans	**18**	**19**	**21**	
		Staphylococcus aureus	**6**	**9**	**11**	**-**

Figure 5. Represents the addition of particles (TiO_2 Anatase) to types of bacteria (S1 *E. coli*, S2 *Streptococcus*, and S3 *Staphylococcus*), (b) Represents the addition of particles (TiO2 Rutile) to types of bacteria (X1 *E. coli*, X2 *Streptococcus*, and X3 *Staphylococcus*).

Table 3 Inhibition zone in mm of (TiO2 Anatase) and (TiO2 Rutile).

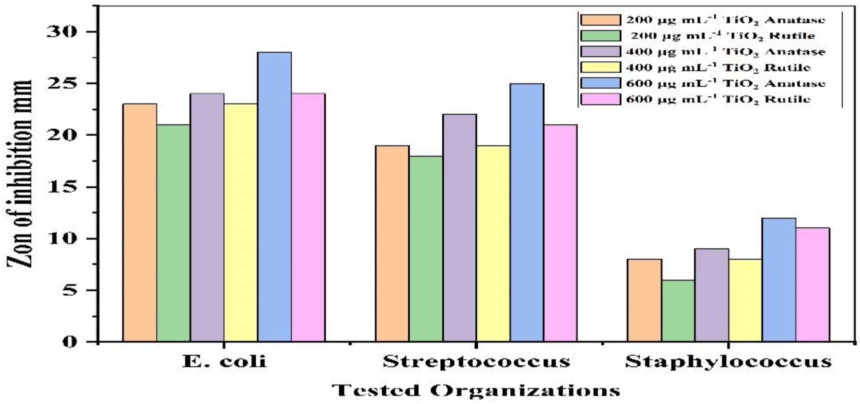

Figure 7. Antibacterial activity of (TiO_2 Anatase) and (TiO_2 Rutile) NPs phase *(E. coli, Streptococcus, and Staphylococcus aureus*) at concentration (200, 400 and 600) µg mL^{-1} by using Well-Diffusion.

Figure (8) shows inhibition areas of (TiO_2 Anatase) and (TiO_2 Rutile) NPs concentrated (600) µg mL^{-1} with amoxicillin (30) µg mL^{-1} using the well-agar diffusion method, using 9 mm blister gel, and the antibacterial activity of TiO_2 NPS. Combines with amoxicillin against *Escherichia coli, streptococci and staphylococci*. The increase in the inhibitory regions was detected due to the synergistic effect of nanoparticles with amoxicillin. The combined effect of amoxicillin nanoparticles is attributed to the degradative effect of the cell wall of amoxicillin and the DNA-binding activity of the nanoparticles [37, 38]. We also note from the figure (7) the inhibition regions space for for Sample (A) representative of TiO_2 Anatase NPs at 600 µg mL^{-1} with amoxicillin (30) µg mL^{-1} shows sensitivity to bacteria (31 mm), (26 mm), and (12 mm) against *E. coli* bacteria (F1), *Streptococcus* (F2) and *Staphylococcus aureus* (F3), respectively About , while on the same bacteria as *E. coli bacteria* (F1), *Streptococcus* (F2) and *Staphylococcus aureus* (F3) shows a fine diffusion assay for (26 mm), (22mm), and (11 mm) respectively In sample B, represented by (TiO_2 Rutile NPs). As shown in the table (4). The activity of TiO_2 NPs was increased with amoxicillin, and a larger concentration of nanoparticles had a better removal effect when combined with amoxicillin. This is because antibiotic molecules and nanoparticles react; nanoparticles have hydroxyl groups, which are readily react with antibiotics. As a result, nanoparticles can be used as antibiotic transporters because of their antibacterial qualities. These findings are consistent with those of Arora et al., who found that TiO_2 nanopartides combined with the antibiotic ceftazidime (CEZ) had a strong synergistic effect against Pseudomonas spp [39]. Furthermore, the antibacterial activity of 8 mm has been demonstrated to be enhanced by TO2 and ZnO nanoparticles against bacteria (S. aureus ATCC 25923) and (E. co-ATCC 25922) [40].

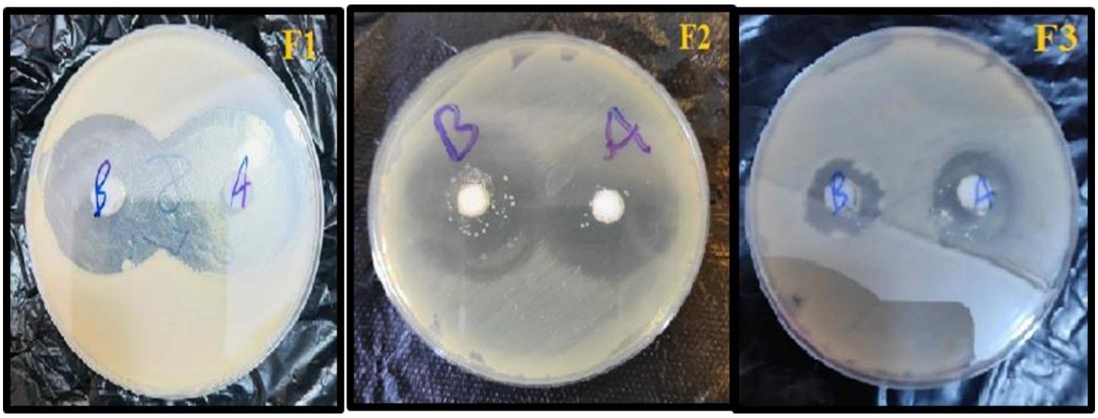

Figure 8. F1 Represents *E. coli* (A-TiO_2Anatase,B-TiO_2 Rutile) , *Streptococcus* (A-TiO_2Anatase,B-TiO2Rutile) and *Staphylococcus aureus* (A-TiO_2Anatase,B- TiO_2 Rutile), at a concentration of 600 µg $mL^{-1.}$

Table 4 Inhibition zone in mm of (TiO_2 Anatase) and (TiO_2 Rutile) NPs with amoxicillin.

Temp.℃	**Phase TiO_2**	**Concentrations, µg mL^{-1}**	**Zone of inhibition, mm**		
			***E. coli* (F1)**	***Streptococcus mutans* (F2)**	***Staphylococcus aureus*(F3)**
650℃	**Anatase & amoxicillin (A)**	**30& 600 amoxicillin**	**31**	**26**	**14**
850℃	**Rutile & amoxicillin (B)**	**30& 600 amoxicillin**	**26**	**22**	**11**

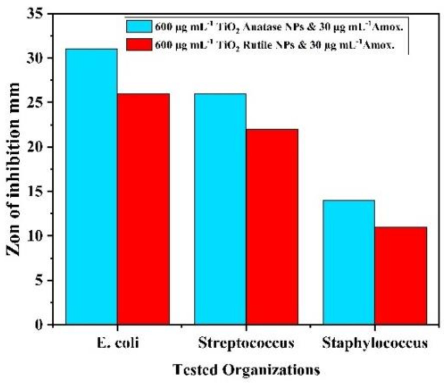

(a)

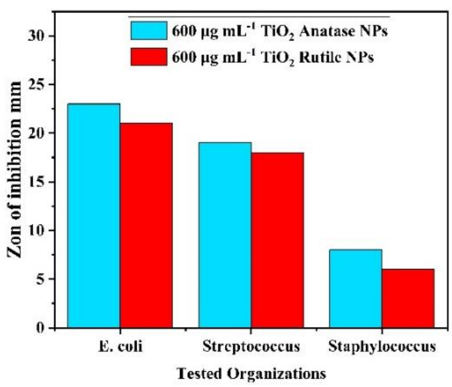

(b)

Figure 9. biological activity of TiO_2Anatase and TiO_2Rutile phase dioxide nanoparticles at a concentration of 600µmL $^{-1}$. (a) pure without amoxicillin (b) with amoxicillin for different types of bacteria (*E. coli – Strptococcus mutans , Staphylococcus*).

4. CONCLUSION

Using $TiCl_4$ as raw material, TiO_2 NPs were successfully produced using the sol-gel method. A comparison of the two phases of TiO_2 NPs is presented in this paper. It was shown that the structural properties of TiO_2NPs depend on the calcination temperature. When the calcination temperature rises, crystallization improves and the size of the crystals increases. Diameter of particles were measured by transmission electron microscopy (TEM), at 850 °C, the statistical distribution of the particle diameters (TiO_2 Rutile) it centered at (37.05) nm, while anatase TiO_2 NPs has a phase diameter of about 15.419 nm at 650 °C. The anatase phase has a sharp peak at 2 = 25.42 and a particle size of 21.4 nm, while the rutile phase has a strong peak at 2 = 27.6 and a particle size of 30.41 nm, according to the Cherry equation. The diameter of the TiO_2 NPs expanded with the increase in the calcination temperature. Due to the stretching mode of the TiO_2 network, FTIR of TiO_2 NPs in the range (400-1000) cm^{-1} revealed Ti-O and Ti-O-Ti bonds. The effect of (TiO_2 anatase) and (TiO_2 rutile) NPs against bacterial strains was seen to rise with NP concentrations due to the decreasing particle sizes of NPs, with the strongest effect reported against *E. coli*. On bacterial cells, the nanoparticles and amoxicillin work together, and the nanoparticles can efficiently boost amoxicillin penetration and absorptionAnatase nanoparticles appeared more efficiently than rutile nanoparticles when used as antisense against bacteria at different concentrations.

REFERENCES

[1] Timothy V. Duncan, "Applications of nanotechnology in food packaging and food safety: barrier materials, antimicrobials and sensors," Journal of colloid and interface science, vol. 363, pp. 1-24, (2011).

[2] Luisa F. and Duncan S., "Nanotechnologies: principles, applications, implications and hands-on activities," Luxembourg: Directorate General for Research and Innovation Industrial technologies (NMP) European Union, (2012).

[3] Trung, T., Won-J. Cho, and Chang-S. Ha. "Preparation of TiO2 nanoparticles in glycerol-containing solutions." Materials Letters 57, no. 18: 2746-2750, (2003).

[4] Han, C. Hwan, Hak-S. Lee, and Sang-D. Han. "Synthesis of nanocrystalline TiO 2 by sol-gel combustion hybrid method and its application to dye solar cells." Bulletin of the Korean Chemical Society 29, no. 8: 1495-1498, (2008).

[5] Haider, J. Adawiya, Zainab N. Jameel, and Samar Y. Taha. "Synthesis and characterization of TiO2 nanoparticles via sol-gel method by pulse laser ablation." Eng. & Tech. Journal 33, no. 5: 761-771, (2015).

[6] Graça M., Silva C., Costa L., and Valente M., "Study of the structural, morphological and electric characteristics of TiO 2 nanopowders," vol. 3, pp. 99-111, (2010).

[7] Carp O., Huisman C. L., and Reller A., "Photoinduced reactivity of titanium dioxide," Progress in solid state chemistry, vol. 32, pp. 33-177, (2004).

[8] Barreca F., Acacia N., Barletta E., Spadaro D., Curro G., and Neri F., "Small size TiO2 nanoparticles prepared by laser ablation in water," Applied Surface Science, vol. 256, pp. 6408-6412, (2010).

[9] Jadhav S., Gaikwad S., Nimse M., and Rajbhoj A., "Copper oxide nanoparticles: synthesis, characterization and their antibacterial activity," Journal of cluster science, vol. 22, pp. 121-129, (2011).

[10] Albukhaty S., Al-Karagoly H., and Dragh M. A., "Synthesis of zinc oxide nanoparticles and evaluated it's activity against bacterial isolates," J. Biotech Res, vol. 11, pp. 47-53, (2020).
[11] Pan Z., Lee W., Slutsky L., Clark R. A., Pernodet N., and Rafailovich M. H., "Adverse effects of titanium dioxide nanoparticles on human dermal fibroblasts and how to protect cells," Small, vol. 5, pp. 511-520, (2009).
[12] Azam A., Ahmed A. S., Oves M., Khan M., and Memic A., "Size-dependent antimicrobial properties of CuO nanoparticles against Gram-positive and-negative bacterial strains," International journal of nanomedicine, vol. 7, p. 3527, (2012).
[13] Podporska J. C., Panaitescu E., Quilty B., Wang L., Menon L., and Pillai S. C.,"Antimicrobial properties of highly efficient photocatalytic TiO2 nanotubes," Applied Catalysis B: Environmental, vol. 176, pp. 70-75, (2015).
[14] Jašková V., Hochmannová L., and Vytřasová J., "TiO2 and ZnO nanoparticles in photocatalytic and hygienic coatings," International journal of photoenergy, vol. 2013, (2013).
[15] Boonen E. and Beeldens A., "Recent photocatalytic applications for air purification in Belgium," Coatings, vol. 4, pp. 553-573, (2014).
[16] Brunette, M. Donald, Pentti T., Marcus T., and Peter T. "Titanium in medicine: material science, surface science, engineering, biological responses and medical applications". Berlin: Springer, (2001).
[17] Martirosyan A. and Schneider Y. J., "Engineered nanomaterials in food: implications for food safety and consumer health," International journal of environmental research and public health, vol. 11, pp. 5720-5750, (2014).
[18] Ko, H. Huey, Hui T. Chen, Feng L. Yen, Wan C. Lu, Chih W. Kuo, and Moo C. Wang. "Preparation of TiO2 nanocrystallite powders coated with 9 mol% ZnO for cosmetic applications in sunscreens." International journal of molecular sciences 13, no. 2: 1658-1669, (2012).
[19] Kenneth S. SUSlick, "Kirk-Othmer encyclopedia of chemical technology," J. Wiley & Sons: New York, vol. 26, pp. 517-541, (1998).
[20] Palmisano L., Augugliaro V., Sclafani A., and Schiavello M., "Activity of chromium-ion-doped titania for the dinitrogen photoreduction to ammonia and for the phenol photodegradation," The Journal of Physical Chemistry, vol. 92, pp. 6710-6713, (1988).
[21] Bessekhouad Y., Robert D., and Weber J. V., "Synthesis of photocatalytic TiO2 nanoparticles: optimization of the preparation conditions," Journal of Photochemistry and Photobiology A: Chemistry, vol. 157, pp. 47-53, (2003).
[22] Sugimoto T., Zhou X., and Muramatsu A., "Synthesis of uniform anatase TiO2 nanoparticles by gel–sol method: 1. Solution chemistry of Ti (OH) n (4− n)+ complexes," Journal of Colloid and Interface Science, vol. 252, pp. 339-346, (2002).
[23] Yu V. Kolen'ko, Churagulov B., Kunst M., Mazerolles L., and Colbeau-Justin C., "Photocatalytic properties of titania powders prepared by hydrothermal method," Applied Catalysis B: Environmental, vol. 54, pp. 51-58, (2004).
[24] Suresh C., Biju V., Mukundan P., and Warrier K., "Anatase to rutile transformation in sol-gel titania by modification of precursor," Polyhedron, vol. 17, pp. 3131-,3135 (1998).
[25] Sánchez-López, E., Gomes, D., Esteruelas, G., Bonilla, L., Lopez-Machado, A. Laura, Galindo, R., Cano, A., Espina, M., Ettcheto, M., Camins, A. and Silva, A.M.,. "Metal-based nanoparticles as antimicrobial agents: an overview". Nanomaterials, 10(2), p.292, (2020).
[26] Han C., Romero N., Fischer S., Dookran J., Berger A., and Doiron A. L., "Recent developments in the use of nanoparticles for treatment of biofilms," Nanotechnology Reviews, vol. 6, pp. 383-404, (2017).

[27] Pandi P. and Gopinathan C., "Structural transformation study of TiO2 nanoparticles annealing at different temperatures and the photodegradation process of eosin-Y," Phase Transitions, vol. 91, pp. 406-425, (2018).
[28] Zaki, H. Neihaya, Amna M. Ali, and Kadhim H. Yaseen. "The evaluation effect of TiO2 nano particles on different bacterial strains isolated from water purification stations in Baghdad." J. Sci 57: 2378-2385, (2016).
[29] Peng T., Zhao D., Dai K., Shi W., and Hirao K., "Synthesis of titanium dioxide nanoparticles with mesoporous anatase wall and high photocatalytic activity," The journal of physical chemistry B, vol. 109, pp. 4947-4952, (2005).
[30] Phromma S., Wutikhun T., Kasamechonchung P., Eksangsri T., and Sapcharoenkun C., "Effect of calcination temperature on photocatalytic activity of synthesized TiO2 nanoparticles via wet ball milling sol-gel method," Applied Sciences, vol. 10, p. 993, (2020).
[31] Rosická D. and Šembera J., "Changes in the nanoparticle aggregation rate due to the additional effect of electrostatic and magnetic forces on mass transport coefficients," Nanoscale research letters, vol. 8, pp. 1-9, 2013.
[32] Al-Nori, T. Majied. "Antibacterial activity of Silver and Gold Nanoparticles against Streptococcus, Staphylococcus aureus and E. coli." Al-Mustansiriyah Journal of Science 23, no. 3, (2012).
[33] Haghi, M., Mohammad H., Mohammad B. Janipour, Saman S. Gholizadeh, M. K. Faraz, Farzad S., and Marjan G. "Antibacterial effect of TiO2 nanoparticles on pathogenic strain of E. coli." International Journal of Advanced Biotechnology and Research 3, no. 3: 621-624, (2012)
[34] de D., Carol L., Matias G. Correa, Fernanda B. Martínez, Camilo S., and Maria J. Galotto. "Antimicrobial effect of titanium dioxide nanoparticles." In Antimicrobial Resistance-A One Health Perspective. London, UK: IntechOpen, (2020).
[35] Ziental, D., Beata Czarczynska-Goslinska, Dariusz T. Mlynarczyk, Arleta Glowacka-Sobotta, Beata S., Tomasz G., and Lukasz S. "Titanium dioxide nanoparticles: prospects and applications in medicine." Nanomaterials 10, no. 2: 387,(2020).
[36] Priyanka, K. Parakkandi, Thiruvangium H. Sukirtha, Kagalagodu M. Balakrishna, and Thomas V. "Microbicidal activity of TiO 2 nanoparticles synthesised by sol–gel method." IET nanobiotechnology 10, no. 2: 81-86, (2016).